Chemical Science

ROYAL SOCIETY OF CHEMISTRY

EDGE ARTICLE

View Article Online
View Journal | View Issue

Cite this: *Chem. Sci.*, 2021, **12**, 9485

All publication charges for this article have been paid for by the Royal Society of Chemistry

Modulation of amyloid-β aggregation by metal complexes with a dual binding mode and their delivery across the blood–brain barrier using focused ultrasound†

Tiffany G. Chan, [abc] Carmen L. Ruehl,[a] Sophie V. Morse, [b] Michelle Simon,[a] Viktoria Rakers,[a] Helena Watts,[bd] Francesco A. Aprile, [a] James J. Choi *[b] and Ramon Vilar *[a]

Received 24th April 2021
Accepted 14th June 2021

DOI: 10.1039/d1sc02273c

rsc.li/chemical-science

One of the key hallmarks of Alzheimer's disease is the aggregation of the amyloid-β peptide to form fibrils. Consequently, there has been great interest in studying molecules that can disrupt amyloid-β aggregation. While a handful of molecules have been shown to inhibit amyloid-β aggregation *in vitro*, there remains a lack of *in vivo* data reported due to their inability to cross the blood–brain barrier. Here, we investigate a series of new metal complexes for their ability to inhibit amyloid-β aggregation *in vitro*. We demonstrate that octahedral cobalt complexes with polyaromatic ligands have high inhibitory activity thanks to their dual binding mode involving π–π stacking and metal coordination to amyloid-β (confirmed *via* a range of spectroscopic and biophysical techniques). In addition to their high activity, these complexes are not cytotoxic to human neuroblastoma cells. Finally, we report for the first time that these metal complexes can be safely delivered across the blood–brain barrier to specific locations in the brains of mice using focused ultrasound.

Introduction

Alzheimer's disease is the most common form of dementia, affecting approximately 50 million people worldwide. One of the key hallmarks of Alzheimer's disease is the accumulation of the amyloid-β (Aβ) peptide in the brain, with post-mortem analyses showing that the total amount of Aβ in Alzheimer's disease brains is significantly higher than in healthy brains. For example, in a patient cohort with an average age of 78 years, previous studies have determined that there was an approximately 3-fold increase in total Aβ in the brains of Alzheimer's disease patients compared to in control patients.[1–3] Aβ is produced *via* the sequential cleavage of the transmembrane protein amyloid precursor protein (APP) by the enzymes β- and γ-secretases.[2,4] The resulting peptides are typically 40 (Aβ1-40) or 42 (Aβ1-42) amino acids in length, and they aggregate over time to form soluble oligomers and insoluble plaques in the extracellular space.[2,4] The presence of these aggregates in the brain ultimately leads to impaired cell signalling, neuronal death and brain atrophy.[5,6]

Cerebral metal ion levels are known to be altered in Alzheimer's disease and it has been proposed that they could play an important role in the pathology of the disease.[7–11] Structural studies have identified a high affinity metal ion binding site at the N-terminal of Aβ (residues 1–16) which can modulate aggregation and the generation of reactive oxygen species upon the binding of endogenous metal ions such as Cu^{2+}, Fe^{3+} and Zn^{2+}.[12–17] Copper(I) is believed to bind to Aβ in a linear two-coordinate fashion through interactions with the histidine residues (His6, His13 and His14), whilst copper(II) is proposed to form square planar complexes with Aβ involving two histidine residues and additional interactions from Asp1 or Ala2.[18–22] Binding to His6, His13 and His14 have also been implicated in the binding of iron(II) and zinc(II) ions to Aβ, but the precise mode of binding remains unclear.[23,24] Numerous studies have shown that the binding of metal ions to Aβ can promote aggregation, resulting in increased neurotoxic effects.[13,14,25,26]

It has been suggested that metal complexes that can preferentially bind to the N-terminal metal ion binding site of Aβ could prove to be therapeutically useful.[27–30] In 2008, Barnham *et al.* reported a series of platinum-based complexes containing 1,10-phenanthroline ligands, which were able to interact with this site and inhibit Aβ aggregation *in vitro*, as well as rescue Aβ-induced

[a]*Department of Chemistry, Imperial College London, White City Campus, 82 Wood Lane, London, W12 0BZ, UK. E-mail: r.vilar@imperial.ac.uk*

[b]*Department of Bioengineering, Imperial College London, London, SW7 2AZ, UK. E-mail: j.choi@imperial.ac.uk*

[c]*Centre of Excellence in Neurotechnology, Imperial College London, London, SW7 2AZ, UK*

[d]*Department of Brain Sciences, Imperial College London, London, W12 0NN, UK*

† Electronic supplementary information (ESI) available. See DOI: 10.1039/d1sc02273c

neurotoxicity in mouse hippocampal slices *ex vivo*.[31] Subsequent experimental and theoretical studies identified the binding mode of these platinum complexes to be *via* π–π stacking with the aromatic residues in the pocket (*e.g.* Tyr10) and coordination to the histidine residues (His6, His13 and His14).[32,33] Since this pioneering study, a handful of other metal complexes have been developed for this application, including cobalt Schiff base complexes reported by Meade *et al.* and iridium benzimidazole complexes reported by Ruiz *et al.*, with promising results being obtained *in vitro*.[34–37] However, as of now, there is just one example of this therapeutic approach being tested *in vivo* as many of these metal complexes are presumed to be either highly toxic or unable to cross the blood–brain barrier (BBB).[36,38]

The presence of the BBB remains one of the biggest obstacles to the successful treatment of brain diseases. To date, the only reported method to open the BBB in a manner that is non-invasive, targeted and transient is the use of focused ultrasound and microbubbles.[39] In this approach, microbubbles followed by the compound of choice are injected intravenously into the bloodstream and the target region is exposed to ultrasound (Fig. S1†). Microbubbles in an ultrasound field radially oscillate, exerting mechanical stress to their surroundings, delivering the compound across the BBB. Focused ultrasound-mediated BBB opening has been used to successfully deliver a wide range of small molecules, antibodies and nanoparticles into the brains of rodents and non-human primates, and the first human clinical trials are currently underway.[40–47]

In this work, we report a series of novel octahedral cobalt(III) salphen and salnaph complexes (Fig. 1) as inhibitors of Aβ aggregation. These complexes were designed to interact with Aβ *via* a dual binding mode involving π–π stacking interactions from the salphen/salnaph ligands and direct coordination *via* the two axial sites on the cobalt. Furthermore, trimethylammonium substituents were added to the ligands to increase water solubility as well as prevent cellular uptake due to the higher hydrophilicity/charge of the resulting complexes. Reduction of cellular permeability would in turn reduce unwanted cytotoxicity. This design was aimed to address some of the limitations of previously reported metal complexes such as high cytotoxicity and low specificity. Through a series of spectroscopic and biophysical experiments, we have shown that these cobalt complexes have high activity as inhibitors of Aβ aggregation through interactions with its N-terminal. Furthermore, the complexes show limited cytotoxicity against human neuroblastoma cells. Following their excellent *in vitro* activity, the most promising cobalt(III)–salnaph complex was successfully delivered across the BBB in both wild-type C57BL/6J and transgenic Alzheimer's disease mice using focused ultrasound-mediated BBB opening methods. Preliminary *in vivo* results indicate that the cobalt(III)–salnaph complex under study is well-tolerated in mice over several weeks with no signs of toxicity observed.

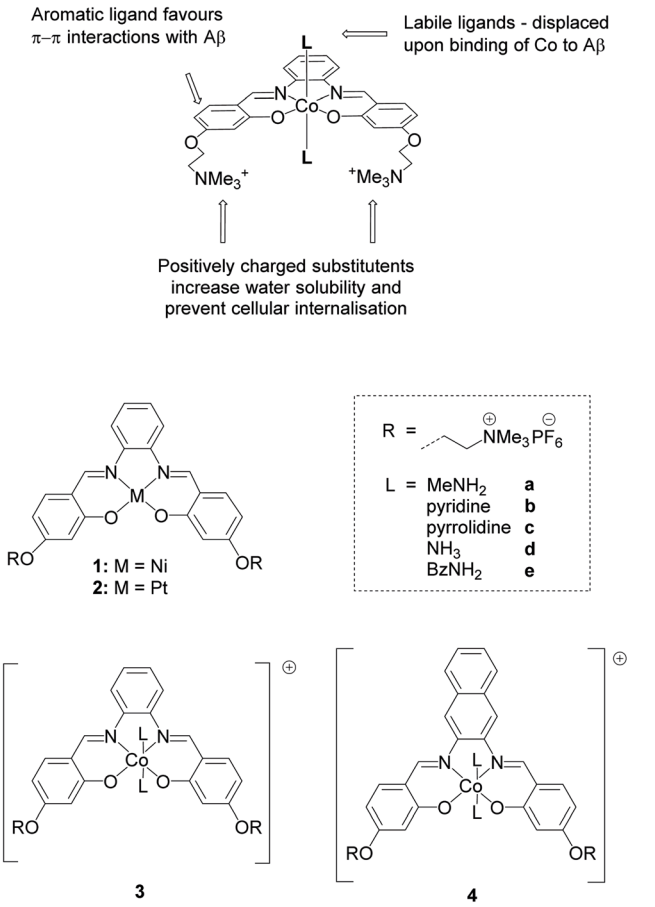

Fig. 1 Structures of metal salphens (**1**, **2** and **3a–3e**) and salnaphs (**4a–4e**) investigated.

Results and discussion

As indicated above, metal complexes that are able to interact with the N-terminal metal binding site of Aβ *via* π–π stacking and/or histidine coordination have been shown to prevent Aβ aggregation *in vitro*.[31,32,34] Inspired by these previously reported examples, we designed and synthesised a series of metal salphens and salnaphs (Fig. 1), and investigated their potential as inhibitors of Aβ aggregation. Our complexes include square planar nickel(II)- and platinum(II) salphen complexes (**1** and **2**) that would only be expected to π–π stack with Aβ, as well as a series of octahedral cobalt complexes (**3a–3e** and **4a–4e**) that, in addition to displaying π–π stacking interactions, were designed to coordinate to the histidine residues of Aβ upon release of their axial ligands. Comparison between the square planar and octahedral salphen complexes (**1** and **2** *vs.* **3a–3e**) allows the effects of coordination to be investigated, whilst comparison between the octahedral salphen and salnaph complexes (**3a–3e** *vs.* **4a–4e**) allows the probing of non-covalent interactions – in particular, π–π stacking. The octahedral complexes were synthesised with a variety of axial ligands to probe any effects related to the different dissociation kinetics of these ligands from the complexes.

Synthesis of metal complexes

Nickel(II) salphen **1** and cobalt(III) salphens **3a** and **3d** were synthesised following a previously reported procedure.[48,49] The new platinum(II) and cobalt(III) salphens **2**, **3b**, **3c** and **3e**, and cobalt(III) salnaphs **4a–4e** were synthesised by first reacting 4-(4-formyl-

3-hydroxyphenoxy)–*N*,*N*,*N*-trimethylethan-1-ammonium bromide with 1,2-phenylendiamine and 2,3-diaminonaphthalene respectively (Scheme 1). Platinum(II) complex **2** was obtained by reacting the salphen ligand with K_2PtCl_4. To form the desired octahedral cobalt complexes, the salphen or salnaph ligand was added to $Co(OAc)_2$, followed by the axial ligand of choice (*i.e.* $MeNH_2$, pyridine, pyrrolidine, NH_3 or $BzNH_2$). Reactions were conducted in air to oxidise the Co^{2+} centre to Co^{3+}.

On successful formation of the desired platinum(II) and cobalt(III) complexes, shifts of the aromatic proton resonances in the ^{1}H NMR spectra were observed. Furthermore, the –OH resonance of the ligand disappeared upon coordination of the metal and, in the case of the cobalt complexes, new peaks corresponding to the attached axial ligands appeared (Fig. S2†). All complexes were fully characterised by ^{1}H NMR spectroscopy, mass spectrometry and elemental analyses.

To investigate the stability of the cobalt(III) complexes (particularly the dissociation of the axial ligand, L), the ^{1}H NMR spectra of complexes **3a–3e** and **4a–4e** were determined in aqueous buffer over time. As shown in Fig. S3,† varying the axial ligand allows for a range of stabilities to be obtained, with complexes **3a**, **3b**, **3d** and **4a**, **4b**, **4d** remaining largely unchanged in aqueous buffer up to 8 h. For complexes **3c**, **3e**, **4c** and **4e**, the axial ligand is lost more rapidly.

Inhibition of Aβ1-42 aggregation

Metal complexes **1**, **2**, **3a–3e** and **4a–4e** were assessed for their ability to inhibit Aβ1-42 aggregation using the Thioflavin-T (ThT) assay. ThT is a benzothiazole dye routinely used to monitor Aβ aggregation that shows strong fluorescence emission when bound to fibrillar structures but low fluorescence emission when free in solution.[50] Complexes were incubated in the presence of 5 μM monomeric Aβ at [Aβ : complex] concentrations ratios = 25 : 1, 20 : 1, 15 : 1, 10 : 1 and 5 : 1 at pH 7.4 and 37 °C for 24 h. The % inhibition by the complexes was determined by measuring the ThT fluorescence at the endpoint of aggregations assuming that decreased fluorescence values indicate a reduced final load of fibrils. As shown in Fig. 2 and S4,† all investigated complexes show a concentration-dependent inhibitory effect. Moreover, this inhibition was greater for octahedral complexes **3a–3e** and **4a–4e** compared to square planar complexes **1** and **2**. This supports the hypothesis that the octahedral cobalt(III) complexes do not interact solely through non-covalent interactions but can also coordinate to Aβ upon release of their axial ligands. Furthermore, the fact that greater than 50% inhibitory activity is observed for all complexes at a [Aβ1-42] : [complex] ratio of 5 : 1 indicates that their interaction with Aβ is strong enough to affect neighbouring Aβ monomers, as well as the Aβ monomer being directly bound to. Similar conclusions were made by Meade *et al.* on the binding of their cobalt(III) Schiff base complexes to Aβ, in which successful inhibition of Aβ aggregation was observed at sub-equimolar ratios in experimental and theoretical studies.[35]

Ideally, the axial ligands attached to cobalt(III) complexes **3a–3e** and **4a–4e** should remain in place until the complex reaches the target location in the brain, but yet be labile enough to allow for efficient coordination to Aβ. As discussed above, we observe

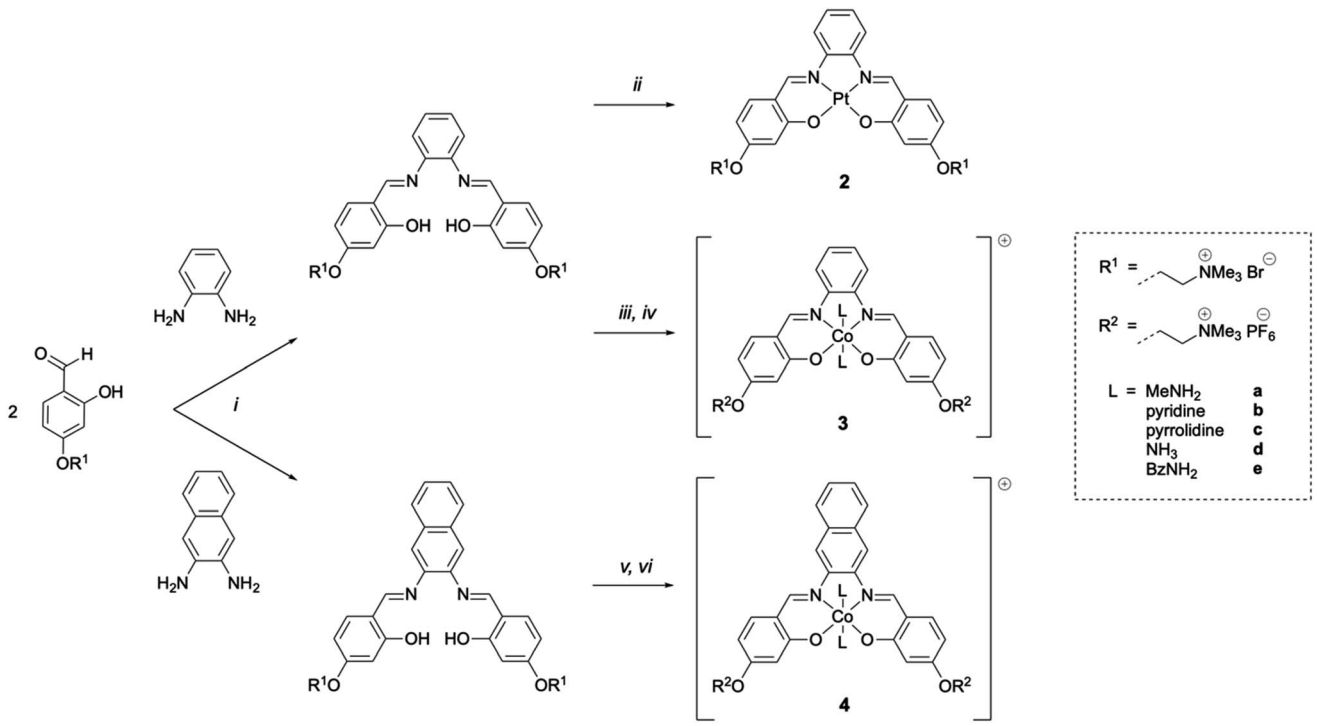

Scheme 1 Synthesis routes to complexes **2**, **3a–3e** and **4a–4e**. [i] EtOH, reflux, 5 h, N_2; [ii] K_2PtCl_4, DMSO, 65 °C, 18 h, N_2; [iii] $Co(OAc)_2 \cdot 4H_2O$, MeOH, r.t., 1 h, N_2; [iv] 10 eq. axial ligand L, aq. sat. NH_4PF_6, MeOH, r.t., 3 h, air; [v] $Co(OAc)_2 \cdot 4H_2O$, MeOH, r.t., 1 min, air; [vi] 10 eq. axial ligand L, aq. sat. NH_4PF_6, MeOH, r.t., 5 h, air.

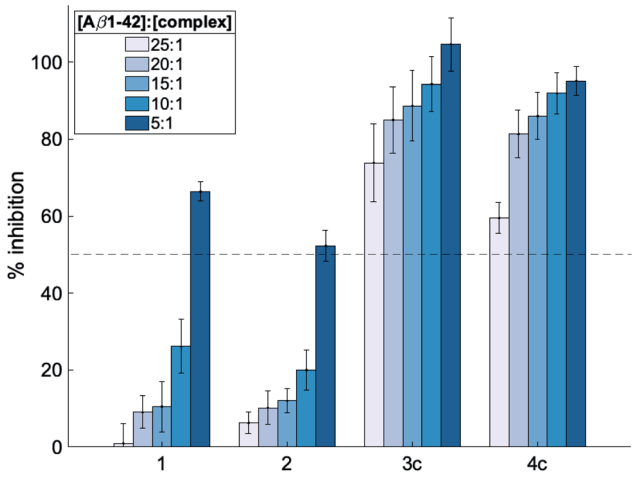

Fig. 2 Inhibition of Aβ1-42 aggregation (%) induced by metal complexes **1**, **2**, **3c** and **4c** determined using the thioflavin-T assay. Complexes were tested at [Aβ42] : [complex] = 25 : 1, 20 : 1, 15 : 1, 10 : 1 and 5 : 1, and all samples were incubated at 37 °C with shaking for 24 h. The dotted line represents the half-inhibition point and all data is reported as the mean ± standard deviation of three independent experiments (see Fig. S4† for inhibition studies with all other metal complexes **3a**, **3b**, **3d**, **3e** and **4a**, **4b**, **4d**, **4e**).

a degree of axial ligand dissociation for all our complexes when dissolved in aqueous buffer (Fig. S3†). The dissociation rate appears to be dependent on the axial ligands attached, with some complexes remaining largely stable for up to 8 h. However, in the presence of Aβ, all complexes **3a–3e** and **4a–4e** show similar behaviour against Aβ aggregation, suggesting that they all undergo axial ligand dissociation and subsequent coordination in the presence of Aβ (Fig. S4†). Due to the similarities in activity between complexes **3a–3e** and **4a–4e**, complexes **3c** and **4c** were selected as representative examples in all subsequent biophysical characterisation.

To confirm that the reduction in fluorescence in Fig. 2 and S4† is linked to the inhibitory strength of the metal complexes, we performed aggregation kinetics at different complex concentrations (using **1**, **3c** and **4c** as representative examples of the complexes under investigation – Fig. 3 and S5†). We normalized the fluorescence data to remove any bias due to potential quenching and only focus on the kinetic aspects of the inhibition (Fig. 3). We found a significant inhibition of the aggregation kinetics for complexes **3c** and **4c**. Noteworthily, this effect is present at sub-stoichiometric concentrations of the metal complexes. On the contrary, complex **1** did not show a significant inhibition at these concentrations, in agreement with the endpoint analyses (Fig. 2).

Regardless of the effects on the kinetics of aggregation, the delta fluorescence values (Fig. S5†) corresponding to the normalized aggregation kinetics in Fig. 3 show that all metal complexes, including compound **1**, lower the ThT fluorescence at the endpoint of aggregation. This result could be because the complexes decrease the final yield of ThT-positive fibrils and/or displace/quench ThT. To assess the extent to which the complexes displace and/or quench ThT, we generated Aβ1-42 fibrils, added ThT, and recorded their fluorescence in the absence and upon addition of 0.1 equivalents of the complexes **1**, **3c**, and **4c** (Fig. S6†). A ∼20% ThT fluorescence reduction by all complexes was observed, indicating that these molecules can interfere with ThT. Nevertheless, this decrease was lower than the one observed in the aggregation kinetics of complexes **3c** and **4c** (∼50%), indicating that the complexes also reduce the final fibril yield. The decrease in fluorescence associated with complex **1** was found to be comparable to ThT displacement/quenching (Fig. S6†).

To verify whether the metal complexes also lower the final yield of fibrils (despite some ThT displacement/quenching), we incubated Aβ1-42 with and without a selection of metal complexes (*i.e.*, **1**, **2**, **3c** or **4c**) at 1 : 1 molar ratio for 48 h at 37 °C and then imaged these samples using negative-stain transmission electron microscopy (TEM) at 52 000× magnification (Fig. S7†). We observed significantly reduced or no fibril formation for all metal complexes which indicates that, at high concentrations (≥ equimolar), the metal complexes can suppress Aβ aggregation *in vitro*. This is true also for complexes **1** and **2**, despite being less effective than **3c** and **4c** at sub-stoichiometric concentrations. These results are consistent with the observations recently reported by Meade *et al.* where they also observed by TEM significant reduction of fibril formation upon addition of cobalt(III) complexes.[37]

Probing binding mode to Aβ

To probe the interactions of the complexes with Aβ, we conducted a series of fluorescence titrations and ^{1}H NMR spectroscopy experiments. The truncated peptide Aβ1-16 is intrinsically fluorescent due to its Tyr10 residue and complexes that interact non-covalently with Aβ *via* π–π stacking are expected to be able to quench this fluorescence.[32,51] To investigate this, the fluorescence emission of the truncated peptide Aβ1-16 was recorded as increasing concentrations of **1**, **3c** and **4c** (as selected examples of the complexes under investigation) were added (0 to 0.75 eq.).

Cisplatin – which can bind to Aβ1-16 *via* coordination with the histidine residues – was included as a negative control.[32] As seen in Fig. 4, minimal quenching effects were observed upon titration with cisplatin which cannot π–π stack with Aβ. In contrast, significant quenching was observed with **1**, **3c** and **4c**, indicating that all these complexes can π–π stack with Aβ as would be expected from their structures. The quenching effect seen is greatest for complex **4c** which has an extended aromatic scaffold.

^{1}H NMR experiments were conducted to probe the interactions between Aβ and the metal complexes further as coordination to Aβ would be expected to strongly perturb the ^{1}H NMR spectrum of Aβ.[32,33] Thus, the ^{1}H NMR spectra of Aβ1-28 with and without our complexes were recorded after 24 h incubation at 37 °C in D_2O : phosphate buffer (1 : 9, pH 7.4). The truncated Aβ1-28 peptide was used instead of the full length peptide as it retains the N-terminal metal ion binding site of interest, whilst being less aggregation-prone.[32,33] On addition of square-planar complexes **1** and **2**, minor perturbations and broadening of

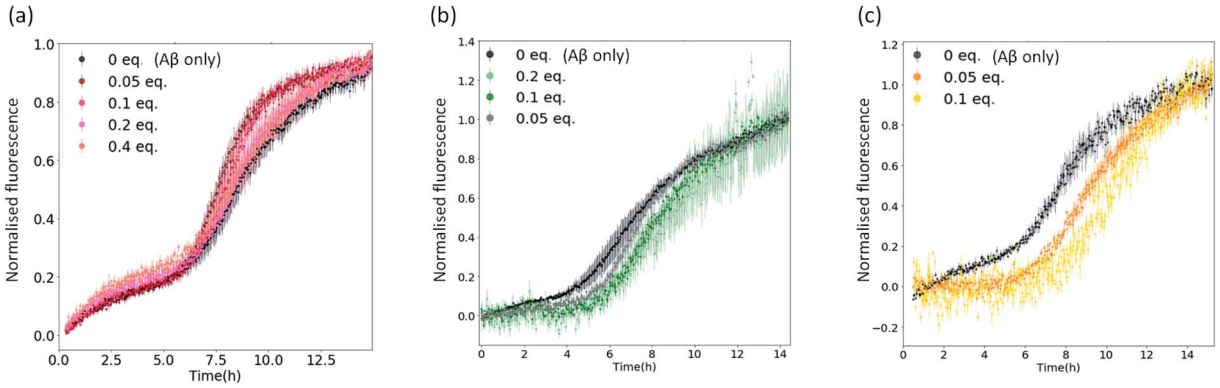

Fig. 3 Plots showing normalised ThT fluorescence over time incubated with 5 μM Aβ and increasing amounts of (a) metal complex **1**; (b) metal complex **3c**; (c) metal complex **4c**.

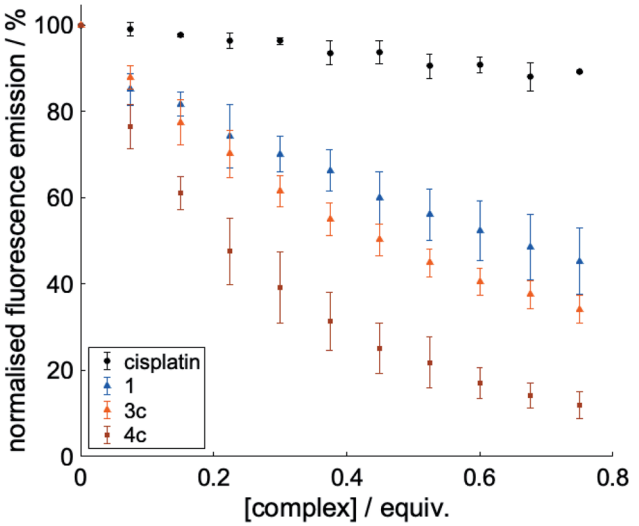

Fig. 4 Normalised fluorescence emission of the Tyr10 residue of Aβ1-16 on addition of cisplatin (negative control), **1**, **3c** and **4c** (0 to 0.75 eq., phosphate buffer, pH 7.4). Quenching is observed with both square planar **1** (blue) and octahedral **3c** and **4c** (orange) complexes. The highest degree of quenching is seen with Co-salnaph complex **4c** (square). All data is reported as the mean ± standard deviation of three independent experiments.

the aromatic signals of Aβ1-28 were observed, which are likely due to π–π stacking effects (Fig. 5; top). In contrast, greater signal broadening was observed when Aβ1-28 was incubated with octahedral complexes **3c** and **4c**, indicating the existence of additional coordination interactions. The Aβ1-28 His signals (see Fig. 5; top) are greatly affected by addition of these cobalt complexes. In addition, new broad signals appear in the region around 6.5 ppm which has been previously associated to Co-His coordination[34] (although it should be pointed out that the complexes **3c** and **4c** have a signal in this region and therefore these resonances cannot be unambiguously assigned).

Computational studies conducted by Heffern *et al.* and Iscen *et al.* on the binding of other octahedral cobalt(III) complexes to Aβ predicted that the most thermodynamically favourable coordination mode to Aβ is coordination to His6 and either His13 or His14.[34,35] To investigate if this was also the case for our complexes, we repeated the ^{1}H NMR experiments with a point-mutated Aβ1-28 peptide in which the His6 residue was replaced by an arginine (H6R mutation). For H6R Aβ1-28, only minor perturbations of the aromatic signals were observed when incubated with any of the metal complexes, suggesting that the His6 residue is key for the binding of the cobalt(III) complexes to Aβ (Fig. 5; bottom).

Cytotoxicity studies

Any compound developed to interact with Aβ should be non-cytotoxic to mammalian cells. To investigate the cytotoxicity *in vitro*, human neuroblastoma cells (SH-SY5Y) were incubated with complex **4b** for 24 h at concentrations up to 100 μM and the resulting cell viability was assessed using the MTS assay. An IC50 of >100 μM was observed in SH-SY5Y cells, making complex **4b** a promising candidate for *in vivo* studies. For comparison, the MTS assay was also performed with complexes **1**, **2**, **3c** and **4c**; the results showed that, like for complex **4b**, these complexes have negligible cytotoxic effects towards SH-SY5Y cells at concentrations up to 20 μM (see Fig. S8†).

In vivo delivery and safety evaluation

For molecules to efficiently cross the BBB and enter the brain, characteristics such as moderate lipophilicity (log *P* of ~2.1), a molecular weight of below 400 Da and a low propensity for hydrogen bond formation are thought to be crucial.[42] Like the majority of the metal complexes previously developed for this application, our complexes have molecular weights greater than 400 Da, making them unlikely to cross the BBB by themselves; thus, in order to ensure that a therapeutic dose of our complexes were delivered to the brain, ultrasound-mediated BBB opening methods were employed.[52] This method was chosen over other BBB delivery methods because drug delivery to the brain can be achieved in a non-invasive, targeted and reversible manner. Since the hippocampal regions of the brain are known to be particularly affected during the early stages of Alzheimer's disease, metal complexes were delivered

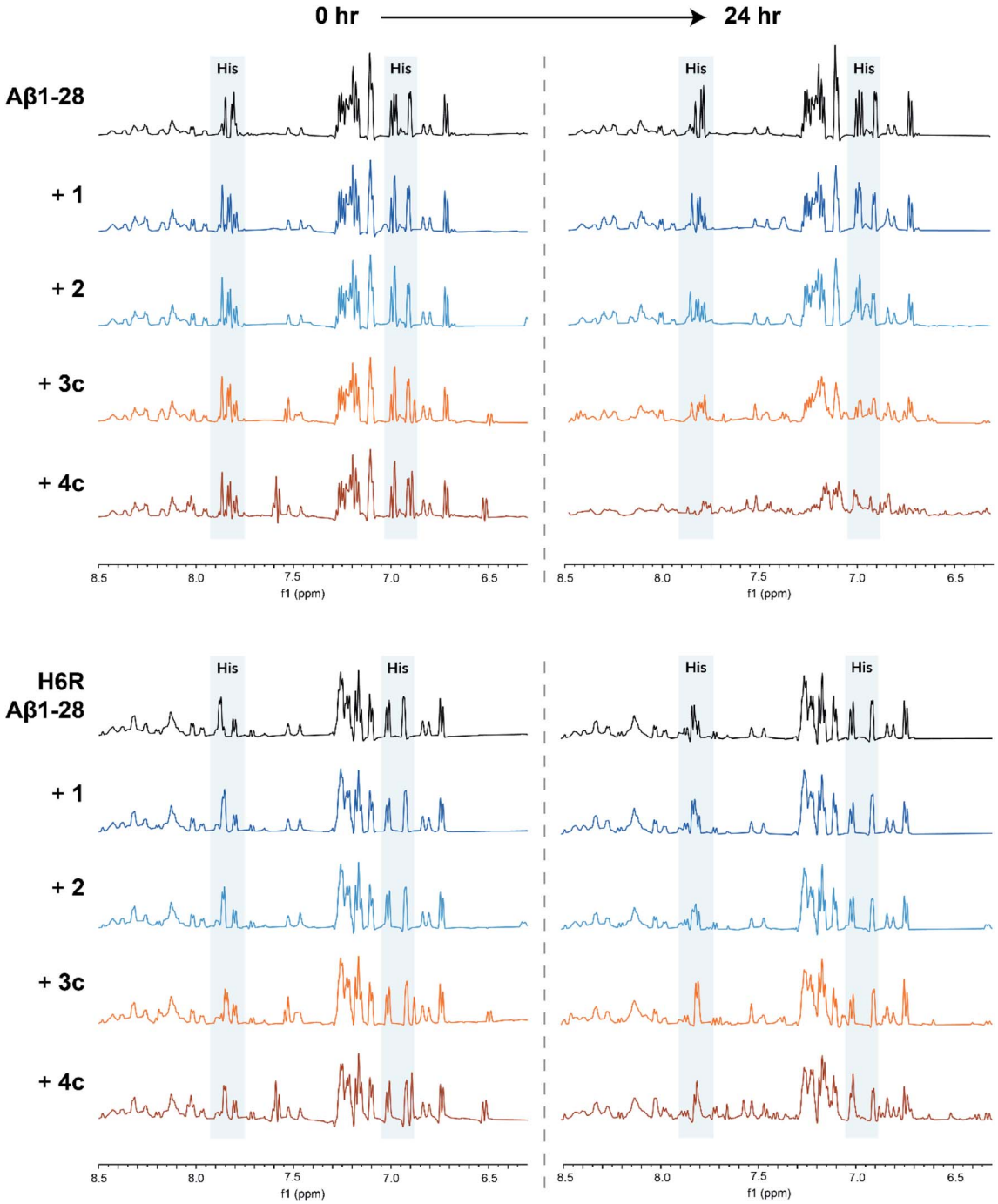

Fig. 5 ^{1}H NMR spectra of Aβ1-28 (top) or H6R Aβ1-28 (bottom) incubated by itself (black), with square planar **1** and **2** (blue) or octahedral **3c** and **4c** (orange) complexes (in a 1-to-1 Aβ-to-complex ratio). All spectra were recorded in D_2O : phosphate buffer (1 : 9, pH 7.4) at 37 °C and the spectra at 0 h and 24 h incubation time are shown. Peaks corresponding to the Aβ histidine residues are highlighted in blue.

specifically to the left hippocampus of mice brains in all experiments, leaving the right hippocampus as our non-ultrasound control.[53]

To prove that we were able to deliver our complexes into the brain using focused ultrasound and microbubbles, the left hippocampus of wild-type C57BL/6J mice (a very commonly used type of laboratory mouse for *in vivo* studies) was sonicated using the ultrasound sequences developed by Morse *et al.* (frequency = 1 MHz; peak-negative pressure = 350 kPa; pulse length = 5 cycles; pulse repetition frequency = 1.25 kHz; burst length = 10 ms; burst repetition frequency = 0.5 Hz).[44] After five ultrasound bursts had been emitted, SonoVue® microbubbles followed by the metal complex of interest (30 mg kg^{-1}) were administered intravenously into the bloodstream. Following transcardial perfusion and fixation, brains were extracted, sectioned, and analysed using laser ablation inductively

coupled plasma mass spectrometry (LA-ICP-MS). For these experiments, the platinum(II)–salphen complex **2** and cobalt(III)–salnaph complex **4c** were used. It should be noted that in the case of the cobalt(III) complex, background detection (due to the endogenous presence of this metal) was expected. The LA-ICP-MS scans show clear ^{195}Pt signal in the left hippocampus (Fig. 6a), corresponding to the injected platinum complex, while no ^{195}Pt signal was observed in the right hippocampus. This shows that complex **2** is unable to cross the BBB by itself as expected, but it can be delivered into the brain using focused ultrasound and microbubbles. Similarly, LA-ICP-MS scans indicate higher accumulation of ^{59}Co (*vs.* background levels of endogenous cobalt) in the sonicated region of the brain (Fig. 6b).

Next, we sought to establish the safety of repeated complex **4b** + ultrasound treatments as Alzheimer's disease patients typically survive for eight to ten years after symptoms begin to show and are therefore likely to require multiple treatments. To assess this, the left hippocampus of wild-type C57BL/6J and transgenic 5xFAD mice (4–5 months old; 5xFAD is a mouse model of Alzheimer's disease which develops amyloid pathology starting from 2 months in age) were sonicated using the same ultrasound sequences as above.[44] After five ultrasound bursts had been emitted, SonoVue® microbubbles followed by complex **4b** (20 mg kg^{-1}; number of mice = 3) were administered intravenously into the bloodstream. Treatment was conducted on a weekly basis over a four-week period with behaviour and body weight monitored throughout. At the study end-point, brains were harvested for post-mortem histological analyses. No changes in behaviour or body weight were detected upon weekly treatment with complex **4b** in either mouse model and no signs of tissue damage were observed in haematoxylin and eosin-stained (H&E) brain sections, indicating that this treatment protocol was well-tolerated (Fig. 7 and S9†).

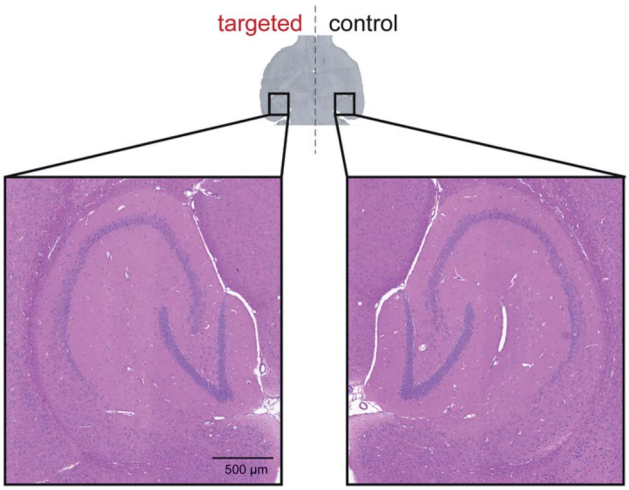

Fig. 7 No signs of tissue damage were observed in H&E-stained sections of brains in which complex **4b** was delivered by sonication.

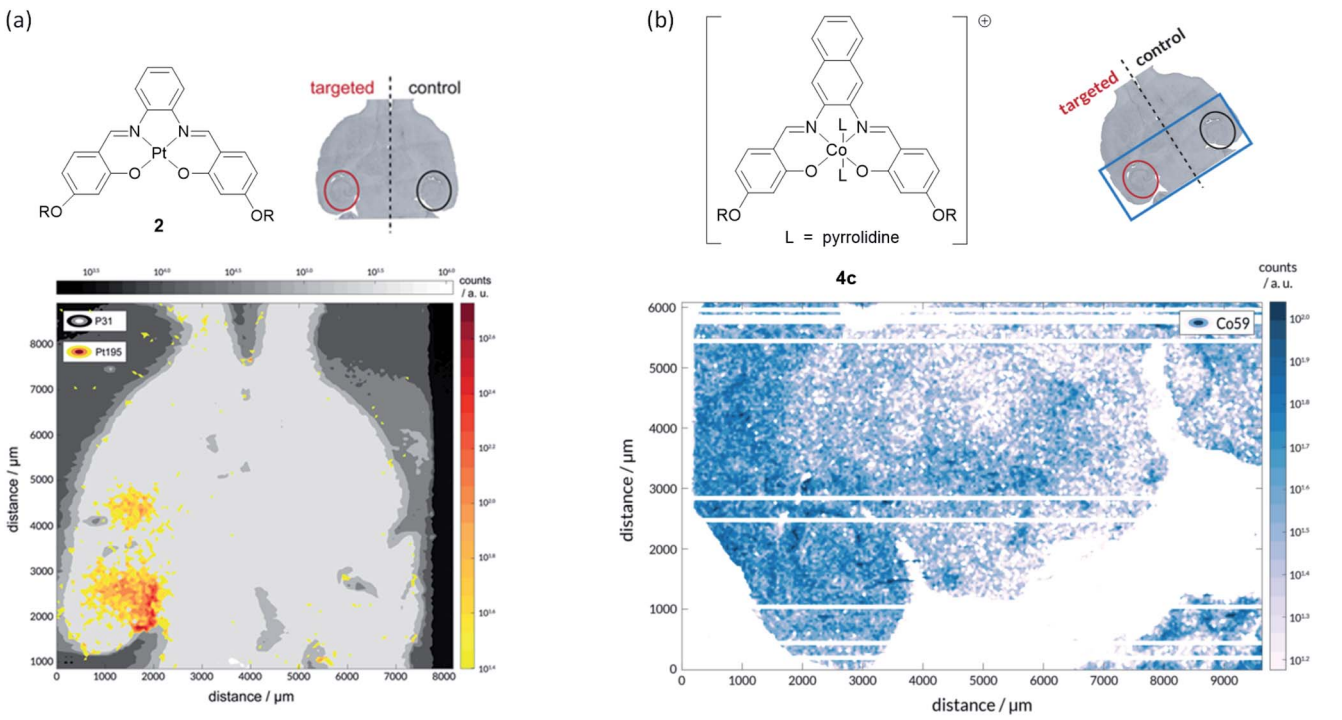

Fig. 6 LA-ICP-MS studies with Pt^{II} and Co^{III} complexes **2** and **4c** respectively. (a) Successful delivery of platinum(II) salphen **2** across the BBB to the left hippocampus is shown by the element distribution map for ^{195}Pt (yellow/red); the image was overlaid on ^{31}P map (grey) to provide brain outline. No evidence of complex accumulation in the right hippocampus (no-ultrasound control), indicating that it does not cross the BBB by itself; (b) successful delivery of cobalt(III) salphen **4c** across the BBB to the left hippocampus is shown by the element distribution map for ^{59}Co (white/blue). A significantly higher concentration of ^{59}Co was detected on the sonicated area.

Conclusions

We have designed and synthesised a series of metal salphen and salnaph complexes that are able to inhibit amyloid beta aggregation *in vitro*. These complexes were designed to overcome some of the limitations of previously reported metal complexes. For example, we report that octahedral cobalt(III) complexes with labile axial ligands have high inhibitory activity against Aβ aggregation due to their dual binding mode involving π–π stacking interactions and direct metal coordination. All our cobalt complexes show a significant inhibition of Aβ aggregation at just 0.1 equivalents of the complex, with the use of 0.2 equivalents completely inhibiting aggregation in most cases. Our metal complexes have minimal cytotoxicity in SH-SY5Y human neuroblastoma cells, making them promising candidates for *in vivo* studies. We also show that these complexes can be successfully delivered across the blood–brain barrier to specific locations in the brains of mice using focused ultrasound and are well-tolerated. To the best of our knowledge, this is the first time that a metal-based compound with *in vitro* inhibitory activity towards Aβ aggregation has been non-invasively delivered across the blood–brain barrier *in vivo*.

Ethical statement

All animal procedures were performed in compliance with the European Directive 63/2010/EU and the UK Animals (Scientific Procedures) Act 1986. All protocols were approved by Imperial College London's Animal Welfare and Ethical Review Body.

Author contributions

T. G. C., C. L. R. and V. R. synthesised the compounds. T. G. C. and M. S. performed spectroscopic and biophysical studies with the compounds and Aβ peptide. T. G. C. and S. V. M. performed the sonication experiments. T. G. C., S. V. M. and H. W. sectioned mice brains and performed histology. T. G. C., F. A. A, J. J. C. and R. V. analysed the data and wrote the manuscript. J. J. C. and R. V. designed the project and raised the funding.

Conflicts of interest

There are no conflicts of interest to declare

Acknowledgements

PhD studentships for T. G. Chan and S. V. Morse were provided by the EPSRC Centre for Doctoral Training in Neurotechnology (EP/L016737/1) and Medical Imaging (EP/L015226/1) respectively. PhD studentships for C. L. Ruehl and V. Rakers were provided by the Department of Chemistry, Imperial College London. The authors would also like to thank Mr P. Haycock (Imperial College London) for NMR assistance, Dr J. Barrit (Imperial College London) for transmission electron microscopy, Mr Barry Sampson (Imperial College London) for LA-ICP-MS assistance. F. A. Aprile thanks UK Research and Innovation (Future Leaders Fellowship MR/S033947/1) and the Alzheimer's Society, UK (grant 511) for support.

References

1 B. R. Roberts, M. Lind, A. Z. Wagen, A. Rembach, T. Frugier, Q. X. Li, T. M. Ryan, C. A. McLean, J. D. Doecke, C. C. Rowe, V. L. Villemagne and C. L. Masters, *Brain*, 2017, **140**, 1486–1498.
2 G. F. Chen, T. H. Xu, Y. Yan, Y. R. Zhou, Y. Jiang, K. Melcher and H. E. Xu, *Acta Pharmacol. Sin.*, 2017, **38**, 1205–1235.
3 W. Xia, T. Yang, G. Shankar, I. M. Smith, Y. Shen, D. M. Walsh and D. J. Selkoe, *Arch. Neurol.*, 2009, **66**, 190–199.
4 P. M. Murphy and H. LeVine, *J. Alzheimer's Dis.*, 2010, **19**, 311–323.
5 L. Pini, M. Pievani, M. Bocchetta, D. Altomare, P. Bosco, E. Cavedo, S. Galluzzi, M. Marizzoni and G. B. Frisoni, *Ageing Res. Rev.*, 2016, **30**, 25–48.
6 L. Crews and E. Masliah, *Hum. Mol. Genet.*, 2010, **19**, R12–R20.
7 M. A. Deibel, W. D. Ehmann and W. R. Markesbery, *J. Neurol. Sci.*, 1996, **143**, 137–142.
8 M. A. Lovell, J. D. Robertson, W. J. Teesdale, J. L. Campbell and W. R. Markesbery, *J. Neurol. Sci.*, 1998, **158**, 47–52.
9 L. M. Miller, Q. Wang, T. P. Telivala, R. J. Smith, A. Lanzirotti and J. Miklossy, *J. Struct. Biol.*, 2006, **155**, 30–37.
10 J. Dong, C. S. Atwood, V. E. Anderson, S. L. Siedlak, M. A. Smith, G. Perry and P. R. Carey, *Biochemistry*, 2003, **42**, 2768–2773.
11 M. W. Bourassa, A. C. Leskovjan, R. V. Tappero, E. R. Farquhar, C. A. Colton, W. E. Van Nostrand and L. M. Miller, *Biomed. Spectrosc. Imaging*, 2013, **2**, 129–139.
12 D. P. Smith, G. D. Ciccotosto, D. J. Tew, M. T. Fodero-Tavoletti, T. Johanssen, C. L. Masters, K. J. Barnham and R. Cappai, *Biochemistry*, 2007, **46**, 2881–2891.
13 M. C. Lee, W. C. Yu, Y. H. Shih, C. Y. Chen, Z. H. Guo, S. J. Huang, J. C. C. Chan and Y. R. Chen, *Sci. Rep.*, 2018, **8**, 4772.
14 F. Hane, G. Tran, S. J. Attwood and Z. Leonenko, *PLoS One*, 2013, **8**, e59005.
15 K. Hensley, N. Hall, R. Subramaniam, P. Cole, M. Harris, M. Aksenov, M. Aksenova, S. P. Gabbita, J. F. Wu, J. M. Carney, M. Lovell, W. R. Markesbery and D. A. Butterfield, *J. Neurochem.*, 1995, **65**, 2146–2156.
16 D. A. Butterfield, T. Reed, M. Perluigi, C. De Marco, R. Coccia, C. Cini and R. Sultana, *Neurosci. Lett.*, 2006, **397**, 170–173.
17 E. Tamagno, M. Guglielmotto, M. Aragno, R. Borghi, R. Autelli, L. Giliberto, G. Muraca, O. Danni, X. Zhu, M. A. Smith, G. Perry, D. G. Jo, M. P. Mattson and M. Tabaton, *J. Neurochem.*, 2008, **104**, 683–695.
18 C. Hureau, V. Balland, Y. Coppel, P. L. Solari, E. Fonda and P. Faller, *J. Biol. Inorg Chem.*, 2009, **14**, 995–1000.
19 T. R. Young, A. Kirchner, A. G. Wedd and Z. Xiao, *Metallomics*, 2014, **6**, 505–517.

20 N. Yako, T. R. Young, J. M. Cottam Jones, C. A. Hutton, A. G. Wedd and Z. Xiao, *Metallomics*, 2017, **9**, 278–291.
21 C. Hureau and P. Dorlet, *Coord. Chem. Rev.*, 2012, **256**, 2175–2187.
22 B. Alies, H. Eury, C. Bijani, L. Rechignat, P. Faller and C. Hureau, *Inorg. Chem.*, 2011, **50**, 11192–11201.
23 B. Alies, A. Conte-Daban, S. Sayen, F. Collin, I. Kieffer, E. Guillon, P. Faller and C. Hureau, *Inorg. Chem.*, 2016, **55**, 10499–10509.
24 F. Bousejra-Elgarah, C. Bijani, Y. Coppel, P. Faller and C. Hureau, *Inorg. Chem.*, 2011, **50**, 9024–9030.
25 P. Faller, C. Hureau and O. Berthoumieu, *Inorg. Chem.*, 2013, **52**, 12193–12206.
26 Y. Miller, B. Ma and R. Nussinov, *Proc. Natl. Acad. Sci. U. S. A.*, 2010, **107**, 9490–9495.
27 D. J. Hayne, S. Lim and P. S. Donnelly, *Chem. Soc. Rev.*, 2014, **43**, 6701–6715.
28 J. M. Suh, G. Kim, J. Kang and M. H. Lim, *Inorg. Chem.*, 2019, **58**, 8–17.
29 H. Liu, Y. Qu and X. Wang, *Future Med. Chem.*, 2018, **10**, 697–701.
30 L. M. F. Gomes, J. C. Bataglioli and T. Storr, *Coord. Chem. Rev.*, 2020, **412**, 213255.
31 K. J. Barnham, V. B. Kenche, G. D. Ciccotosto, D. P. Smith, D. J. Tew, X. Liu, K. Perez, G. A. Cranston, T. J. Johanssen, I. Volitakis, A. I. Bush, C. L. Masters, A. R. White, J. P. Smith, R. A. Cherny and R. Cappai, *Proc. Natl. Acad. Sci. U. S. A.*, 2008, **105**, 6813–6818.
32 G. Ma, F. Huang, X. Pu, L. Jia, T. Jiang, L. Li and Y. Liu, *Chem.–Eur. J.*, 2011, **17**, 11657–11666.
33 I. Sasaki, C. Bijani, S. Ladeira, V. Bourdon, P. Faller and C. Hureau, *Dalton Trans.*, 2012, **41**, 6404–6407.
34 M. C. Heffern, P. T. Velasco, L. M. Matosziuk, J. L. Coomes, C. Karras, M. A. Ratner, W. L. Klein, A. L. Eckermann and T. J. Meade, *ChemBioChem*, 2014, **15**, 1584–1589.
35 A. Iscen, C. R. Brue, K. F. Roberts, J. Kim, G. C. Schatz and T. J. Meade, *J. Am. Chem. Soc.*, 2019, **141**, 16685–16695.
36 G. S. Yellol, J. G. Yellol, V. B. Kenche, X. M. Liu, K. J. Barnham, A. Donaire, C. Janiak and J. Ruiz, *Inorg. Chem.*, 2015, **54**, 470–475.
37 K. F. Roberts, C. R. Brue, A. Preston, D. Baxter, E. Herzog, E. Varelas and T. J. Meade, *J. Inorg. Biochem.*, 2020, **213**, 111265.
38 M. C. Heffern, V. Reichova, J. L. Coomes, A. S. Harney, E. A. Bajema and T. J. Meade, *Inorg. Chem.*, 2015, **54**, 9066–9074.
39 K. Hynynen, N. McDannold, N. Vykhodtseva and F. A. Jolesz, *Radiology*, 2001, **220**, 640–646.
40 J. J. Choi, K. Selert, F. Vlachos, A. Wong and E. E. Konofagou, *Proc. Natl. Acad. Sci. U. S. A.*, 2011, **108**, 16539–16544.
41 J. Park, Y. Zhang, N. Vykhodtseva, F. A. Jolesz and N. J. McDannold, *J. Controlled Release*, 2012, **162**, 134–142.
42 L. H. Treat, N. McDannold, Y. Zhang, N. Vykhodtseva and K. Hynynen, *Ultrasound Med. Biol.*, 2012, **38**, 1716–1725.
43 K. C. Wei, P. C. Chu, H. Y. J. Wang, C. Y. Huang, P. Y. Chen, H. C. Tsai, Y. J. Lu, P. Y. Lee, I. C. Tseng, L. Y. Feng, P. W. Hsu, T. C. Yen and H. L. Liu, *PLoS One*, 2013, **8**, e58995.
44 S. V. Morse, A. N. Pouliopoulos, T. G. Chan, M. J. Copping, J. Lin, N. J. Long and J. J. Choi, *Radiology*, 2019, **291**, 459–466.
45 T. G. Chan, S. V. Morse, M. J. Copping, J. J. Choi and R. Vilar, *ChemMedChem*, 2018, **13**, 1311–1314.
46 A. Abrahao, Y. Meng, M. Llinas, Y. Huang, C. Hamani, T. Mainprize, I. Aubert, C. Heyn, S. E. Black, K. Hynynen, N. Lipsman and L. Zinman, *Nat. Commun.*, 2019, **10**, 4373.
47 N. Lipsman, Y. Meng, A. J. Bethune, Y. Huang, B. Lam, M. Masellis, N. Herrmann, C. Heyn, I. Aubert, A. Boutet, G. S. Smith, K. Hynynen and S. E. Black, *Nat. Commun.*, 2018, **9**, 2336.
48 V. Rakers, P. Cadinu, J. B. Edel and R. Vilar, *Chem. Sci.*, 2018, **9**, 3459–3469.
49 C. L. Ruehl, A. H. M. Lim, T. Kench, D. J. Mann and R. Vilar, *Chem.–Eur. J.*, 2019, **25**, 9691–9700.
50 H. Naiki, K. Higuchi, M. Hosokawa and T. Takeda, *Anal. Biochem.*, 1989, **177**, 244–249.
51 C. D. Syme, R. C. Nadal, S. E. J. Rigby and J. H. Viles, *J. Biol. Chem.*, 2004, **279**, 18169–18177.
52 W. M. Pardridge, *J. Cereb. Blood Flow Metab.*, 2012, **32**, 1959–1972.
53 Y. Mu and F. H. Gage, *Mol. Neurodegener.*, 2011, **6**, 85.